Optimal Path Planning and Control of Assembly Robots for Hard-Measuring Easy-Deformation Assemblies

An Wan, Jing Xu, *Member, IEEE*, Heping Chen, *Senior Member, IEEE*, Song Zhang, and Ken Chen

***Abstract*—Assembly robots are widely used in the electronics and automotive industries. However, assembly robots still face formidable challenges for assembling large-scale heavy-weight components such as the tail of the plane. First, the large-scale component is difficult to measure; thus, the optimal assembly path is difficult to obtain. To this end, a learning from demonstration-based optimal path planning method is developed and implemented. Second, the deformation caused by a heavy-weight component will lead to a large motion error and could cause damage to the component. To solve this problem, a Gaussian process regression (GPR)-based deformation prediction and compensation method is presented to improve the robot motion accuracy. The simulation results show that the proposed GPR-based deformation compensation method can achieve high accuracy. An experimental prototype was developed to evaluate the proposed methods, and the results demonstrate the effectiveness of the proposed methods. Therefore, the proposed methods provide a path toward hard-measuring easy-deformation assembly task.**

***Index Terms*—Easy deformation, Gaussian process regression (GPR), hard measuring, learning from demonstration (LfD).**

I. Introduction

AT PRESENT, assembly robots are widely used in industries such as electronics, appliances, and automotive [1]–[4]. With improvements in the positioning accuracy and load capacity of robots, it becomes possible for assembly robots to perform assembly of heavy-weight components. Because assembly robots could greatly improve the assembly quality of large-scale components and are able to adapt to different components with different sizes and weights, which can considerably decrease the number of assembly fixtures and reduce the cost, such robots have been widely investigated [5]–[7].

However, compared to the assembly of electronics, automobiles, household appliances, and other light-weight components, the automated robotic assembly of large-scale heavy-weight components still faces two major challenges:

A. Challenge 1

How to accurately plan the optimal assembly path. That is, to know where to go for the assembled component.

Prior to assembly, we have to accurately measure the relative position and orientation (pose) between fixed and moving components. In other words, the target pose of the moving component (assembly path) is required to be planned, which is generally obtained by measuring the axis of the fixed hole [8]. Due to its high precision and large measurement range, a laser tracker is typically used for measuring the hole axis. However, due to the large scale and complex shape, the measurement distance will be very far and the measurement laser will be easily blocked; thus, it is difficult to directly obtain the hole axis in large-scale heavy-weight component assembly. To this end, the learning from demonstration (LfD, also called programming by demonstration) method is used to obtain the assembly path in this paper, in which the robot learns the experience from a human operator and performs the assembly using the experience [9]–[10]. Nehmzow *et al.* [11] proposed an LfD method to teach a robot to follow human behaviors, and then the robot transfers human behaviors to robot control code using system identification techniques. Aleotti *et al.* [12] improved a virtual environment-based programming method, where the robot is programmed by a human operator wearing a data glove in a virtual environment. The recognized task was performed in a simulated environment before being performed in a real environment to supervise and validate the learning process, making the demonstration easier and more effective.

In the existing LfD-based methods, human behaviors are recorded and transferred to robot control code, and then the robot simply repeats the human operator's behaviors. However, in hard-measuring easy-deformation assembly, the assembled component is difficult to be handled for teaching. Moreover, because the human assembly path is not optimal, it is unreasonable

Manuscript received October 8, 2016; revised December 22, 2016 and February 3, 2017; accepted February 15, 2017. Date of publication February 17, 2017; date of current version August 14, 2017. Recommended by Technical Editor H. Qiao. This work was supported in part by the National Science Foundation of China under Grant 51675291 and Grant U1613205, and in part by the Fund of the State Key Laboratory of Tribology of China under Grant SKLT2015B10. *(Corresponding author: Jing Xu.)*

A. Wan, J. Xu, and K. Chen are with the State Key Laboratory of Tribology and the Department of Mechanical Engineering, Tsinghua University, Beijing 100084, China (e-mail: 07wanan07@163.com; jingxu@tsinghua.edu.cn; kenchen@tsinghua.edu.cn).

H. Chen is with the Ingram School of Engineering, Texas State University, San Marcos, TX 78746 USA (e-mail: heping.chen@txstate.edu).

S. Zhang is with the School of Mechanical Engineering, Purdue University, West Lafayette, IN 47907 USA (e-mail: szhang15@purdue.edu).

Color versions of one or more of the figures in this paper are available online at http://ieeexplore.ieee.org.

Digital Object Identifier 10.1109/TMECH.2017.2671342

for the robot to directly repeat the human demonstration. To this end, we propose an LfD-based optimal assembly path planning method. A small and light demonstration peg is inserted into the fixed hole by a human operator, and the assembly process is recorded by a real-time measurement sensor; then, the optimal assembly path is planned by the robot for real peg assembly. Here, the robot learns the human experience (i.e., the optimal assembly path) rather than simply repeats the human assembly path.

B. Challenge 2

How to deal with the deformation caused by the heavy-weight component. That is, to know how to deal with the assembled component.

During assembly, deformation of the robot caused by the heavy-weight component cannot be neglected. Thus, we have to utilize the measured results and control strategy to achieve high-precision pose adjustment regardless of the deformation. Compared with small component assembly, the heavy weight of the assembled component (the assembled component typically weighs a few tons) would cause a serious deformation, resulting in jamming or damage [13]. The unknown value and distribution of the weight make accurately modeling the deformation difficult. Moreover, increasing the stiffness to compensate for deformation would make the mechanical structure bulky.

To overcome the problem of deformation, Takahashi *et al.* [14] presented a passive alignment principle-based control strategy to perform compliance control by using contact force detection with a force sensor, which can achieve extremely high precision in a ring and shaft assembly. However, in easy-deformation assembly, it is impossible for a force sensor to detect the tiny contact force due to the heavy-weight payload, leading to damage to the assembled component. Another solution is to rebuild the robot kinematics, but this solution would fail due to the unknown value and distribution of the weight. Cheah *et al.* [15] proposed an approximate Jacobian control method to address the uncertainty of robot kinematics, and this method does not require the exact kinematics and Jacobian matrix of the robot. This method works well for point control, but it is only applicable for point control; thus, it is not suitable for trajectory control of assembly tasks. Cheng *et al.* [16] improved an adaptive neural network tracking control method to address the uncertainty of kinematics, but this method does not perform well if singular points exist; hence, it is not reliable in practice. A robust nonlinear control method using three-layer neural networks was also presented to control the motion of the manipulator without an exact kinematics model [17]. This method requires considerable computation and is thus difficult to be realized in real time, which is required for the real-time control of assembly robots. In addition, H. Chen *et al.* [18], [19] proposed a robotically controlled holographic optical tweezers method to transport biological cells, where a drag force model and gradient descent optimization based method was improved to calibrate cell dynamics online. But this method is not suitable for large component control.

Qiao *et al.* [20]–[22] improved a high-precision peg-in-hole assembly strategy based on the concept of attractive region in environment and analysis of the allowable range of the peg system, where contact forces are used to control the robot, replacing some of the input forces. The method allows the relative low-precision robot to perform high-precision peg-in-hole assembly. But in this method, the peg needs to contact with the hole, which would damage the assembled component in heavy-weight component assembly. Cheng *et al.* [23] proposed an online assembly parameter optimization method for high-precision robot assembly process, using Gaussian process regression (GPR) surrogated Bayesian optimization algorithm (GPRBOA) to optimize peg-in-hole assembly process parameters. Wu *et al.* [24] further improved an orthogonal exploration (OE-GPRBOA) method based on the GPRBOA, using the OE method to improve the searching efficiency. Chen *et al.* [25] improved a robot learning method based on GPR to optimize the assembly parameters in complex robot assembly process such as three stage torque converter assembly, where the GPR is used to model the relationship between the assembly parameters and system performance.

These GPR-based methods aim to optimize the assembly parameters using GPR model and various optimization algorithms, depending on force control and force sensor. However, as mentioned above, in easy-deformation assembly, it is impossible for a force sensor to realize high-precision control. Therefore a high-precision control method without using force sensor and force control has to be investigated. In this paper, we propose a learning based online robot control method that uses GPR and deformation compensation strategy to model and compensate the robot deformation. The proposed method can predict and compensate the deformation without knowing the value and distribution of the weight of the assembled component in advance or rebuilding the robot kinematics, leading to a great improvement in the robot motion accuracy.

In short, the main contribution of this paper is to develop innovative technologies to perform hard-measuring easy-deformation assembly by proposing an LfD-based optimal path planning method and a GPR-based deformation prediction and compensation method to improve the robot motion accuracy.

II. Working Principle

A. Assembly Robot System

The proposed assembly robot system consists of a real-time three-dimensional (3-D) measurement sensor (such as a vision sensor, laser tracker, or other real-time 3-D sensors), an assembly robot, and a computer (see Fig. 1). The assembly robot generally has six degrees of freedom (DOF), and the assembled component is mounted on the robot end effector. In hard-measuring easy-deformation assembly, the hole is the fixed component and the peg is the moving component. In the proposed assembly system, a real-time 3-D vision sensor is adopted. Therefore, there are several markers on the demonstration peg and the real assembled peg, and the marker locations with respect to the peg axis have been calibrated in advance. The overall assembly process is described as follows (see Fig. 2).

First, a small and light demonstration peg with the same fit tolerance as the real peg is inserted into the fixed real hole, and the human assembly process is recorded by the real-time

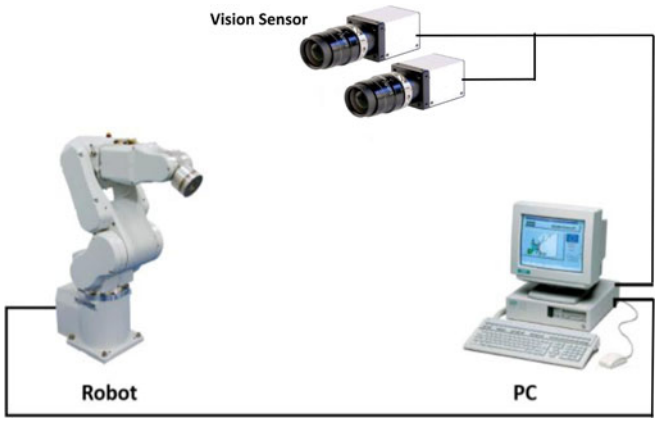

Fig. 1. Assembly robot system.

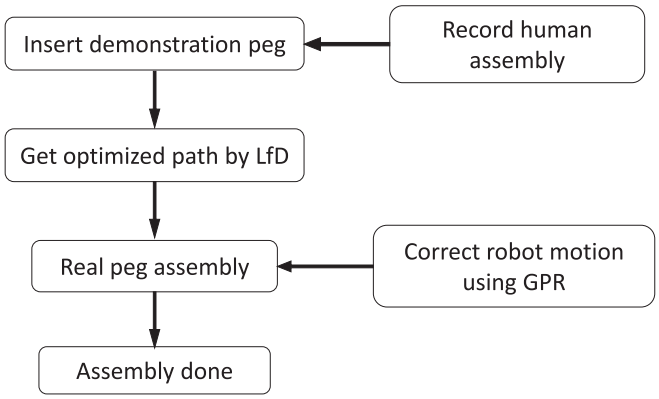

Fig. 2. Assembly process.

3-D vision sensor. Obviously, the human assembly path is not optimal, even with jamming.

Second, the human assembly path is optimized using the LfD method to obtain the optimal assembly path, which is collinear to the fixed hole axis.

Third, the real peg is moved along the optimal assembly path. The assembly process is also monitored by the real-time 3-D vision sensor, and the robot motion path is corrected using the GPR-based deformation prediction and compensation method until the assembly process is complete.

B. LfD-Based Optimal Path Planning Method

Prior to assembly, the optimal assembly path is required to avoid jamming and damage to the assembly component. To this end, an LfD-based optimal path planning method is proposed for hard-measuring easy-deformation assembly in this paper. The principle and procedure are described as follows.

The human operator assembles a small and light demonstration peg into the fixed hole as a demonstration. Then, the assembly process is recorded by a real-time 3-D vision sensor to teach the robot. Because there is no assisted force or position sensor to restrict manual assembly, the assembly cannot achieve high precision along the assembly path without jamming; hence, it is not effective for the robot to directly repeat the manual assembly path. To simplify the optimization of the manual assembly path, the human operator is asked to rotate the demonstration

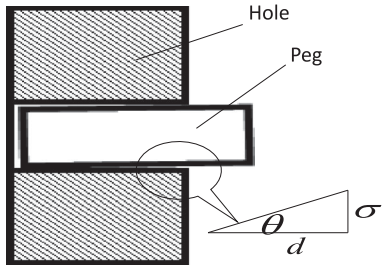

Fig. 3. Maximum inclined angle and insertion distance.

peg along the hole axis to reach the maximum inclined angle because it is impossible for the human operator to keep the axis of the demonstration peg collinear to that of the hole.

Then, the robot learns and plans the optimal assembly path (the hole axis) by using the following optimal path planning method.

Assume that the maximum clearance (the acceptable maximum assembly error) between the peg and hole is σ and that the distance the peg has entered into the hole is d. Then, the maximum inclined angle θ is a function of the insertion distance d (see Fig. 3).

$$\theta = \frac{\sigma}{d}. \tag{1}$$

Clearly, the maximum inclined angle θ decreases with the increased insertion distance of the demonstration peg; thus, the maximum inclined angle θ of the demonstration peg is becoming increasingly smaller.

Obviously, the angle θ is also the angle between the peg axis $\vec{v}_p$ and the hole axis $\vec{v}_h$. Hence, we have

$$\vec{v}_p \cdot \vec{v}_h = \cos\theta. \tag{2}$$

During the assembly procedure, there will be several groups of peg axes $\vec{v}_p$ and the corresponding maximum inclined angle θ, composing an n-by-3 matrix V_p and an n-by-1 matrix ϕ. Due to the measurement error, there is no perfect vector $\overrightarrow{v_h}$ that can fit the above equation for every peg position. Thus, we obtain a least squares problem. Set an objective function

$$M = \sum_{i=1}^{n} \left(V_{pi} \cdot \overrightarrow{v_h} - \cos\theta_i\right)^2. \tag{3}$$

The least squares problem is to find an optimal $\overrightarrow{v_h}$ to minimize the objective function. Because the problem can be expressed in matrix form, the least squares problem has a closed-form solution. Calculate the pseudoinverse of the matrix V_p

$$\text{pinv}(V_p) = (V_p^T V_p)^{-1} V_p^T. \tag{4}$$

Then, the optimal hole axis $\vec{v}_h$ can be obtained by a closed-form solution

$$\vec{v}_h = (V_p^T V_p)^{-1} V_p^T \cos\phi. \tag{5}$$

The obtained hole axis $\vec{v}_h$ is the desired optimal assembly path.

In practical assembly, the robot generally moves along a given assembly path, which determines a series of the assembled component positions. However, to insert the peg into the hole, a correct orientation is also required (see Fig. 4). Note that the peg is

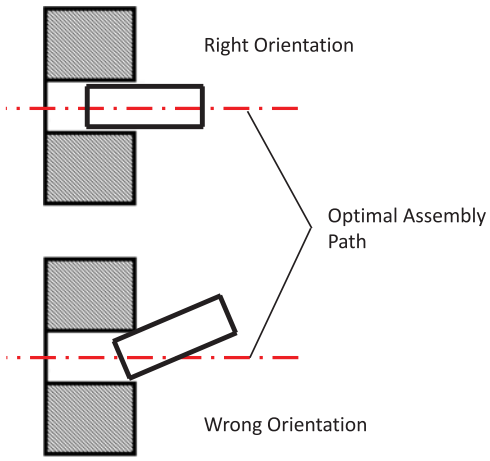

Fig. 4. Correct orientation versus incorrect orientation.

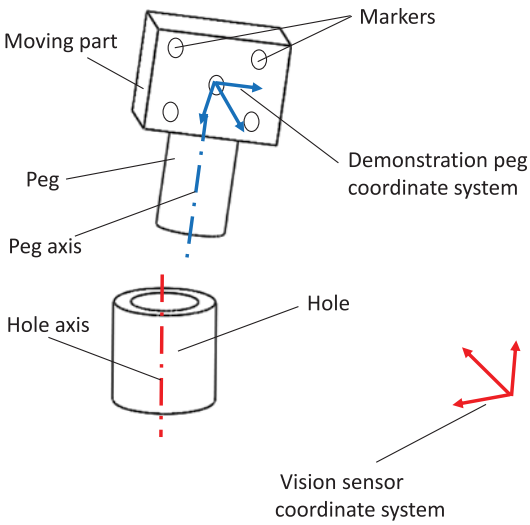

Fig. 5. Demonstration peg coordinate system.

expected to move along the hole axis throughout the peg-in-hole assembly procedure. Therefore, only the position of the peg is varied during the assembly process, while the orientation of the peg is constant. Clearly, the peg axis must coincide with the optimal assembly path.

Here, we can construct a demonstration peg coordinate system P_{xyz} using the markers on the demonstration peg as shown in Fig. 5, and the peg axis can be described in this coordinate system. The next step is to find an orientation of P_{xyz} to allow the demonstration peg axis to coincide with the obtained optimal assembly path. Set the real-time 3-D vision sensor coordinate system as VS_{xyz}. Set the rotation matrix from P_{xyz} to VS_{xyz} as R. Then, we have the following constraint:

$$\vec{v}_h = R \cdot \vec{v}_{pp} \tag{6}$$

where $\vec{v}_h$ is the optimal assembly path in VS_{xyz} and $\vec{v}_{pp}$ is the peg axis in P_{xyz}, which is calibrated in advance. Here, R is a 3-by-3 matrix with 3 unknown rotation angles; however, there is

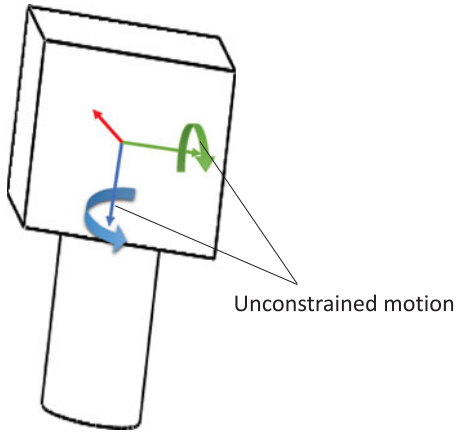

Fig. 6. Unconstrained motion.

only one constraint equation for determining the demonstration peg orientation. In other words, the peg can rotate along the optimal assembly path and turn upside down along any axis that is perpendicular to the optimal assembly path, as shown in Fig. 6. To solve this problem and simplify the measurement, the markers are allowed to completely face the real-time 3-D vision sensor, which restricts the other two direction rotations of the demonstration peg, that is, the desired orientation can be determined.

At this point, the optimal assembly path is learned and planned by using the proposed LfD-based optimal path planning method. The proposed method does not require exact alignment of the peg and hole, and the demonstration is easy to perform without an additional force sensor or position sensor.

C. GPR-Based Deformation Prediction and Compensation Method

After obtaining the optimal assembly path, the next step is to control the assembled component moving along the planned optimal assembly path. The heavy-weight component inevitably results in deformation of the robot. To improve robot motion accuracy, a GPR-based deformation prediction and compensation method is proposed in this paper.

D. Establish the GPR Model

The assembled component is mounted on the robot end effector. To establish the GPR-based deformation prediction and compensation model, we control each robot joint to move to different angles, and the corresponding poses of the assembled component are measured by the real-time 3-D vision sensor. Comparing the measured poses with the theoretical poses of the assembled component, we can obtain N groups of deformation, which are set to be the output of training data Y. A 6-by-N matrix X composed of N groups of the six joint angles is considered as the input of training data.

Set a process function $f(x)$ between the input X and output Y. Define a Gaussian process $f(x) \sim GP(m(x), k(x, x'))$, where $m(x)$ and $k(x, x')$ are the mean function and covariance

function of $f(x)$, respectively. Then, we have

$$m(x) = E[f(x)] \tag{7}$$

$$k(x, x') = E[(f(x) - m(x)) \cdot (f(x') - m(x'))] \tag{8}$$

where $x, x' \in R^d$ are random variables.

The robot motion error and measurement error cannot be ignored. The process function is

$$y = f(x) + \varepsilon \tag{9}$$

where x and y are samples of X and Y, respectively, and ε is the error. To construct a Gaussian process, the error ε is assumed to obey the Gaussian distribution $\varepsilon \sim N(0, \sigma_n^2)$, where σ_n^2 represents the integrated error of X and Y.

Thus, we can obtain the prior distribution of output Y according to the input X:

$$Y \sim N(0, G) \tag{10}$$

in which $G = K(X, X) + \sigma_n^2 I_n$ is the covariance function of the distribution, where $K(X, X) = K_n = (k_{i,j})$ and $k_{i,j} = k(x_i, x_j)$ presents the correlation between the two elements x_i and x_j of the input X. For the test input, its predicted output is subject to the joint probability distribution. Then, for a new input x^*, the distribution of the corresponding output y^* is

$$\begin{bmatrix} Y \\ y^* \end{bmatrix} \sim N\left(0, \begin{bmatrix} K(X, X) + \sigma_n^2 I_n & K(x, x^*) \\ K(x^*, x) & k(x^*, x^*) \end{bmatrix}\right) \tag{11}$$

where $K(x, x^*)$ is the covariance matrix of X and x^*, and we have $K(x, x^*) = K(x^*, x)^T$. Therefore, the above distribution is a joint probability distribution of Y and y^*. Then, the posterior distribution of the output y^* is

$$y^* | X, y, x^* \sim N(\bar{y}^*, \mathrm{cov}(y^*)) \tag{12}$$

in which

$$\bar{y}^* = K(x^*, x) G^{-1} y \tag{13}$$

$$\mathrm{cov}(y^*) = k(x^*, x^*) - K(x^*, X) G^{-1} K(X, x^*) \tag{14}$$

E. Train the GPR Model

The reliability of the GPR model depends on the covariance function, and the training of the GPR model consists of searching for the optimal mean and covariance function. A commonly used covariance function is the square exponential function, which has the following form:

$$k(x, x') = \sigma_f^2 \exp\left(-\frac{1}{2}(x - x')^T M^{-1} (x - x')\right) \tag{15}$$

where $M = \mathrm{diag}(l_i^2)$, l_i^2 is the variance scale, and σ_f^2 is called the signal variance [26]–[28]. Thus, we obtain a hyper-parameter $\theta = \{M, \sigma_f^2, \sigma_n^2\}$, which describes the character of the input and output of the GPR model. Therefore, the GPR training consists of optimizing θ by the training data.

The optimal θ is generally obtained using the likelihood method. First, set a likelihood function $L(\theta) = -\log(p(Y | X, \theta))$, in which $p(Y | X, \theta)$ is the conditional probability of the output Y. Typically, the likelihood function is of the following form:

$$L(\theta) = \frac{1}{2} Y^T C^{-1} Y + \frac{1}{2} \log |C| + \frac{n}{2} \log 2\pi \tag{16}$$

where $C = K_n + \sigma_n^2 I_n$.

Second, calculate the partial derivatives of $L(\theta)$, through which we obtain

$$\frac{\partial L(\theta)}{\partial \theta_i} = \frac{1}{2} tr((\alpha\alpha^T - C^{-1}) \frac{\partial C}{\partial \theta_i}) \tag{17}$$

where $\alpha = C^{-1} Y = (K + \sigma_n^2 I_n)^{-1} Y$.

Finally, the optimal hyper-parameter is obtained by minimizing the partial derivatives using the steepest descent method.

At this point, the optimal hyper-parameter and the covariance function are obtained. Then, given a new input, we can predict the output using the trained GPR model.

F. Online GPR-Based Deformation Compensation Method

Prior to assembly, the real-time 3-D vision sensor measures the manual assembly procedure to obtain the optimal assembly path. The assembled component is mounted on the robot end effector. Then, the robot is controlled to move in space, and the assembled component poses are measured by the real-time 3-D vision sensor; meanwhile, several groups of joint angles are also recorded. Taking into account the deformation caused by the heavy-weight component, the measured pose M cannot completely coincide with the theoretical pose T, and the deformation is

$$\varepsilon = M - T. \tag{18}$$

Considering N groups of joint angles J and deformations ε as the input and output of the GPR model, we can train the GPR model using the above method. Then, given a new joint angle, we can predict the deformation using the GPR model. To reach the target pose T regardless of robot deformation, the following control strategy is performed.

First, calculate the corresponding joint angles using the inverse kinematics

$$J_0 = \mathrm{ikine}(T). \tag{19}$$

However, taking into account the robot deformation, the assembled component cannot reach the target pose only by robot kinematics. By setting the joint angles J_0 to be the new input, the deformation ε_0 can be predicted by the GPR model

$$\varepsilon_0 = \mathrm{GPR}(J_0). \tag{20}$$

Second, the adjusted pose by robot motion is

$$Tp_1 = T - \varepsilon_0. \tag{21}$$

Third, we can obtain the adjusted joint angles using the inverse kinematics

$$J_1 = \mathrm{ikine}(Tp_1). \tag{22}$$

Finally, the actual pose of the assembled component is

$$AP_1 = Tp_1 + \varepsilon_1 \tag{23}$$

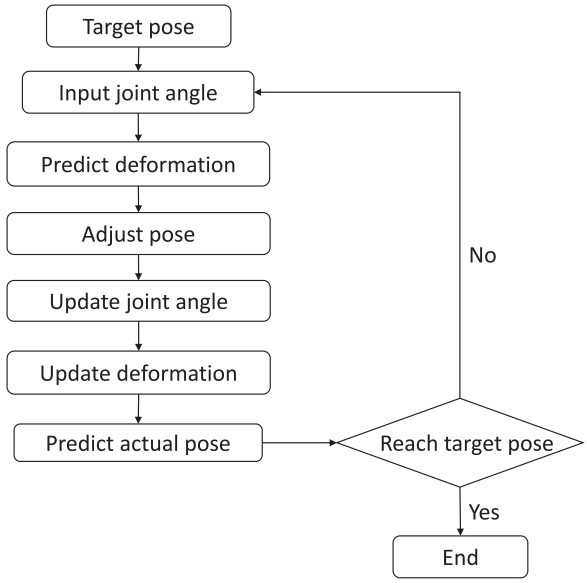

Fig. 7. Flowchart of GPR-based control method.

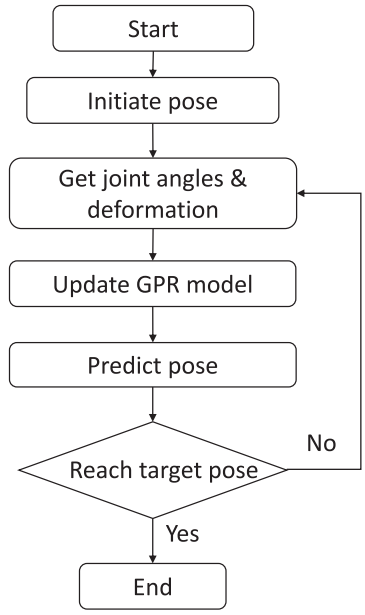

Fig. 8. Flowchart of dealing with jam control strategy.

where $\varepsilon_1 = \mathrm{GPR}(J_1)$ is the deformation corresponding to the joint angles J_1. Here, $J_1 \neq J_0$; therefore, we have to determine whether AP_1 is equal to T. Calculate the corresponding Euler angles α, β, γ and translation vector $\overrightarrow{v}$ of the matrixes AP_1 and T. Setting two thresholds k_1 and k_2, if $\left|(\alpha_i, \beta_i, \gamma_i)^T - (\alpha_T, \beta_T, \gamma_T)^T\right| > k_1$ or $\left|(x_i, y_i, z_i)^T - (x_T, y_T, z_T)^T\right| > k_2$, we should perform the next prediction using the new initiate joint angles J_1 and deformation ε_1.

$$Tp_2 = T - \varepsilon_1 \tag{24}$$

$$J_2 = \mathrm{ikine}(Tp_2) \tag{25}$$

$$AP_2 = Tp_2 + \varepsilon_2. \tag{26}$$

The process iterates until $\left|(\alpha_i, \beta_i, \gamma_i)^T - (\alpha_T, \beta_T, \gamma_T)^T\right| < k_1$ and $\left|(x_i, y_i, z_i)^T - (x_T, y_T, z_T)^T\right| < k_2$, and the assembled component can be considered to reach the target pose T.

Finally, control the robot movement to the joint angles J_i, and the assembled component will reach the target pose. Fig. 7 shows the entire iteration procedure. Note that the iteration is calculated by the computer, and the robot does not move until the iteration is completed and the final joint angles are obtained; therefore, the control process is very efficient.

G. Jam Handling Method

During the assembly procedure, the pose of the assembled component should be monitored to avoid jams. The real-time 3-D vision sensor measures the pose of the assembled component at every target point along the planned assembly path. For the ith target pose, the measured pose M_i is compared with the predicted pose P_i. If the difference $m_i = M_i - P_i$ is greater than a given threshold, it means that the deformation prediction has a noticeable error, which would lead to a high risk of jams. Therefore, the deformation must be predicted again using the newest training data.

The jam handling method is performed by controlling the assembled component to move back to the pose P_{i-1} and performing another iteration (see Fig. 8).

First, obtain the first group of joint angles using the above method, and then control the robot to move to the predicted pose AP_1. The actual pose M_1 is obtained by the vision sensor.

Second, the deformation $\varepsilon_1 = M_1 - Tp_1$ and the joint angles J_1 are added to the GPR training data to predict the next pose AP_2. Similarly, the actual pose M_2 is obtained, and the GPR model is updated. The process iterates until the error $(M_i - T)$ is smaller than the given threshold.

Throughout the assembly procedure, the deformation is predicted by the GPR method without modeling the kinematics after deformation. Therefore, the proposed deformation prediction and compensation method is suitable for different assembly systems and payload conditions with high accuracy and efficiency.

III. Simulations

To test the proposed GPR method, we perform the following simulations.

A. Cantilever Beam

Set a cantilever beam as shown in Fig. 9, where point P represents the assembled component, and its position changes with the angle θ. Consequently, we have the following kinematics:

$$\begin{cases} x = L \cdot \cos\theta \\ y = L \cdot \sin\theta. \end{cases} \tag{27}$$

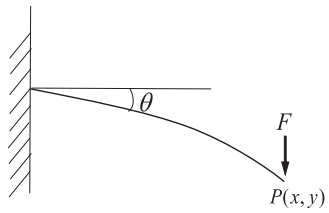

Fig. 9. Cantilever beam.

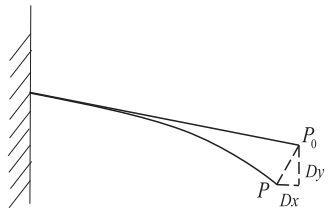

Fig. 10. Deformation of the cantilever beam.

Taking into account gravity acting on the assembled component, the deformation cannot be ignored. Set the material to be aluminum, and the elasticity modulus is $E = 71$ GPa. Set the link length to be $L = 500$ mm and the width and height of the cross section to be $b = 30$ mm and $h = 50$ mm, respectively. Set the gravity acting on the assembled component to be $F = 1000$ N. Then, by ignoring the gravity acting on the cantilever beam and tensile deformation, for each joint angle, we can obtain the deformation of point P (shown in Fig. 10).

$$\begin{cases} Dx = -\dfrac{F \cdot \cos\theta \cdot L^3}{3E(bh^3/12)} \cdot \sin\theta \\ Dy = -\dfrac{F \cdot \cos\theta \cdot L^3}{3E(bh^3/12)} \cdot \cos\theta. \end{cases} \tag{28}$$

Given several joint angles θ, we can obtain several positions of point P and the corresponding deformation D. Then, we add measurement error to obtain the measured values M and measured deformation mD. Here, the measurement error is set to be approximately 10 μm. The GPR model can now be constructed by the input θ and output mD. To test the GPR model, we randomly set ten new input joint angles α and calculate the theoretical deformation D_α. Then, we place the new input α into the GPR model to obtain the predicted deformation D_p. Finally, the two groups of deformations are compared to obtain the prediction error of the GPR model.

$$\mathrm{ER} = D_p - D_\alpha. \tag{29}$$

Table I presents the simulation results. As shown in this table, the prediction error is approximately 10 μm, which is close to the measurement error. Fig. 11 shows the prediction error at different joint angles, and as shown, the prediction error is very stable and has no relation with the joint angles.

B. Assembly Robot System

We set an assembly robot using the parameters of the ABB IRB 120 robot (i.e., the robot kinematics). Then, given a set of joint angles J, we can obtain the theoretical terminal pose P_T using the theoretical robot kinematics. Taking into account the deformation caused by the assembled part, we obtain the actual terminal pose P_A. Therefore, the deformation is $D = P_A - P_T$. Due to the measurement error, the measured pose P_M is not equal to the actual pose, and the measured deformation is $D_M = P_M - P_T$, which is the output of the GPR training data.

In the proposed control system, the input and output of the GPR model are the joint angles and deformation, respectively. To train the GPR model, we set the robot to move 40 poses in space, and the deformations are measured by the vision sensor. Then, the GPR model is trained by the 40 groups of training data.

To test the effectiveness of the system, let the robot randomly move to 10 poses, obtaining 10 groups of joint angles J_o. By placing J_o into the GPR model, we can obtain the predicted deformation D_P. Finally, the predicted deformation D_P is compared with the actual deformation D to obtain the prediction error. Here, the measurement error of the vision sensor is set to be 10 μm.

Table II presents the simulation results, in which position deformation (PD) and orientation deformation (OD) are the position and orientation deformation and ER_P and ER_O are the position and orientation prediction error. As shown in this table, the prediction error is considerably less than the deformation. Figs. 12 and 13 show the position prediction error and orientation prediction error at different joint angles. As shown, the prediction error is very stable. Hence, the proposed GPR method can reach high accuracy, and it is highly versatile.

TABLE I
DEFORMATION AND PREDICTION ERROR OF CANTILEVER BEAM

α/rad	D_x/mm	D_y/mm	ER_x/mm	ER_y/mm
0.003	−7.511	0.020	0.011	0.011
0.213	−7.175	1.552	0.018	0.018
0.290	−6.898	2.056	0.016	0.014
0.556	−5.419	3.367	0.017	0.012
0.833	−3.399	3.739	0.018	0.015
0.929	−2.692	3.602	0.017	0.017
0.933	−2.663	3.593	0.017	0.013
1.074	−1.705	3.146	0.014	0.018
1.518	−0.021	0.398	0.013	0.020
1.570	0.000	−0.051	0.014	0.012

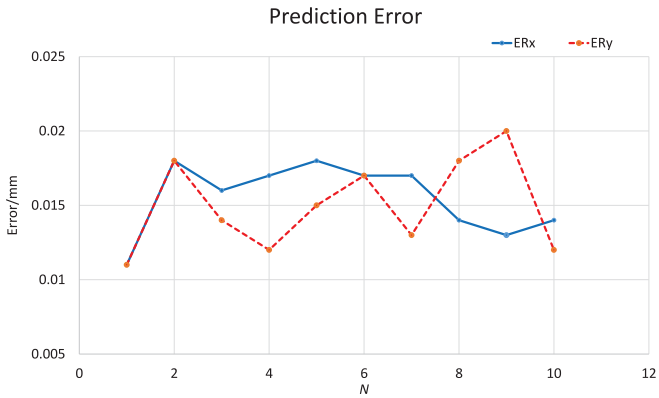

Fig. 11. Prediction error in two directions.

TABLE II
DEFORMATION AND PREDICTION ERROR OF ASSEMBLY ROBOT

Pose	PD/μm	OD/″	ER$_P$ /μm	ER$_O$ /″
1	103.1	209.8	16.2	13.6
2	96.0	185.8	14.7	13.1
3	94.7	163.1	16.0	13.6
4	90.2	181.0	14.9	13.2
5	99.8	196.0	22.6	18.0
6	94.1	141.9	12.8	11.4
7	52.6	91.2	16.2	13.8
8	95.5	176.6	17.8	14.8
9	98.5	197.2	21.7	17.2
10	81.8	156.4	17.5	15.0

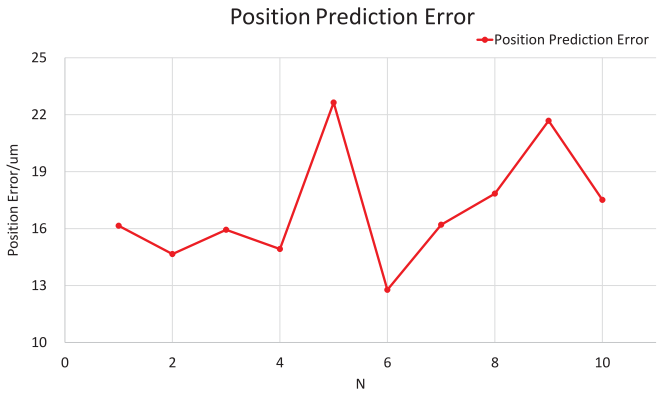

Fig. 12. Position prediction error.

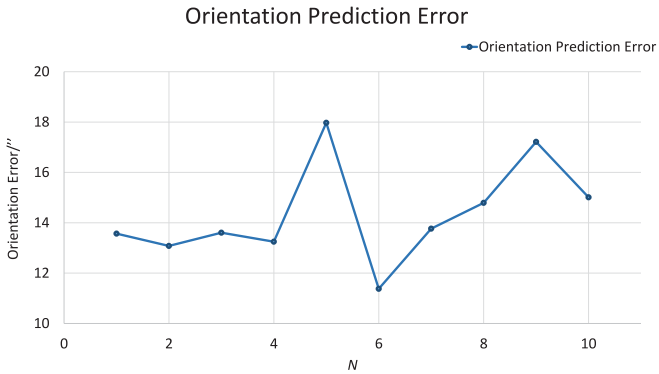

Fig. 13. Orientation prediction error.

IV. EXPERIMENTAL

Fig. 14 shows the proposed assembly robot system. Here, the assembly robot is ABB IRB 120, whose maximum payload is 3 kg. The real-time 3-D vision sensor consists of two cameras, whose resolution is 2560 × 2480. The assembled component is designed to be close to the maximum payload of the robot; therefore, the assembly task can be considered to be hard-measuring and easy-deformation. The hole is 40 μm larger than the peg in diameter; thus, the accepted maximum assembly error is 40 μm, which exceeds the robot motion accuracy.

A laser tracker is used to verify the effectiveness of the proposed GPR method. As shown in Fig. 14, the laser tracker measures reflectors mounted on the assembled component to obtain

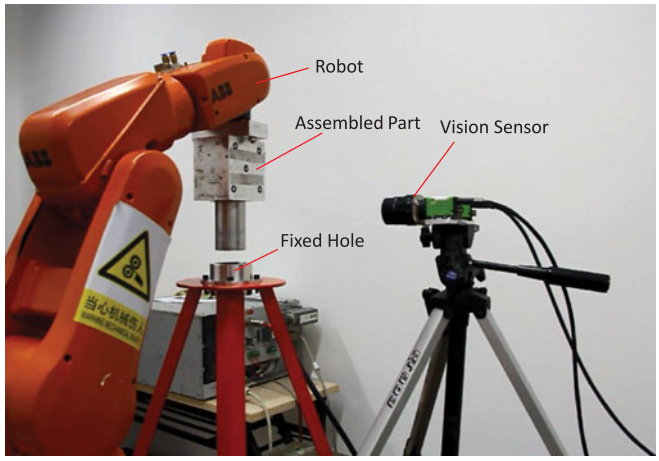

Fig. 14. Experiment system.

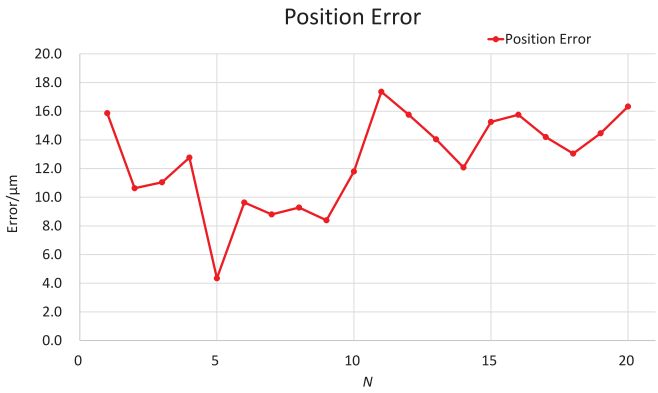

Fig. 15. Position prediction error of GPR.

the pose of the assembled component. Here, the laser tracker (Leica AT901) works at a distance of approximately 1 m, and the measurement accuracy is within 20 μm [29], [30].

By controlling the robot to move to several poses in space, the poses of the assembled component are measured by the laser tracker. Then, several groups of joint angles and the corresponding deformations are obtained. The GPR model can be trained by setting the joint angles to be the input and deformations to be the output. The robot is then controlled to move to 20 new locations, and the robot joint angles J and deformations ε are obtained. Then, the new joint angles J are input to the GPR model to obtain the predicted deformations ε_p. Finally, the prediction error is obtained by comparing ε_p with ε.

Figs. 15 and 16 show the position error and orientation error. As shown, the position error is approximately 10–20 μm, which is close to the measurement error, and the orientation error is approximately 10–20 arcsec, which is approximately 5–10 μm offset at a distance of 100 mm. Thus, the experiment verifies that the proposed GPR method can achieve high accuracy and satisfy the requirements for hard-measuring easy-deformation assembly.

As shown in Fig. 14, the hole and the real-time 3-D vision sensor are fixed on the platform. The markers on the demonstration peg are tracked by the real-time 3-D vision sensor through-

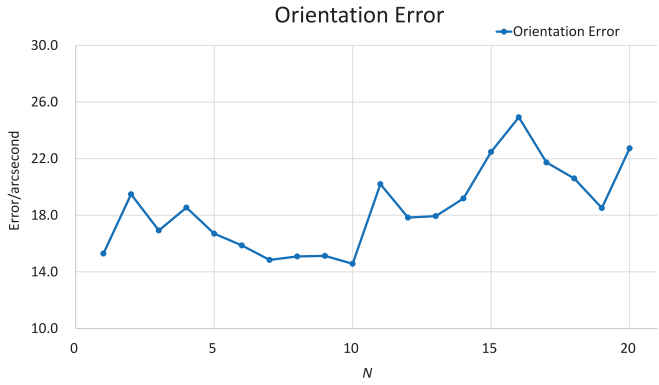

Fig. 16. Orientation prediction error of GPR.

out the demonstration procedure to obtain the peg axis in the field of view of the real-time 3-D vision sensor. After the human operator performs the assembly demonstration, the optimal assembly path is learned and planned by the robot system using the proposed path planning method. Next, the assembled peg is mounted on the robot end effector, and then the practical assembly is performed along the planned assembly path.

The assembly procedure is monitored by the real-time 3-D vision sensor, and the robot motion is controlled by the above GPR-based deformation prediction and compensation method. The result indicates that the robot follows the obtained assembly path very well, and the assembly process is successful, proving that the obtained assembly path is the optimal one due to the tiny acceptable assembly error.

V. Conclusion

This paper presents an assembly robot system used for hard-measuring easy-deformation assembly.

To perform the assembly, an LfD-based optimal path planning method is developed. A real-time 3-D vision sensor is used to record the human operator assembly procedure, and an optimal assembly path is learned and planned from the human demonstration. Because the robot will deform during the assembly process caused by the heavy-weight component, a GPR-based deformation prediction and compensation method is proposed to handle the deformation without knowing the exact value and distribution of the weight of the assembled component. The proposed methods are validated through experiments and simulations. The results demonstrate that the proposed methods can be used to perform hard-measuring easy-deformation assembly, which will significantly reduce the assembly cycle time, mitigate the risk of component damage and decrease assembly cost.

References

[1] H. X. Wei, J. D. Tan, and T. M. Wang, "Sambot: A self-assembly modular robot system," *IEEE Trans. Mechatronics*, vol. 16, no. 4, pp. 745–757, Aug. 2011.

[2] B. S. Kim, J. S. Park, C. Moon, G. M. Jeong, and H. S. Ahn, "A precision robot system with modular actuators and MEMS micro gripper for micro system assembly," *J. Mech. Sci. Technol.*, vol. 22, pp. 70–75, Jan. 2008.

[3] R. A. Knepper, T. Layton, J. Romanishin, and D. Rus, "IkeaBot: An autonomous multi-robot coordinated furniture assembly system," in *Proc. 2013 IEEE Int. Conf. Robot. Autom.*, 2013, pp. 855–862.

[4] G. Reinhart, J. Werner, and F. Lange, "Robot based system for the automation of flow assembly lines," *Prod. Eng.-Res. Develop.*, vol. 3, pp. 121–126, Mar. 2009.

[5] S. Jorg, J. Langwald, J. Stelter, G. Hirzinger, and C. Natale, "Flexible robot-assembly using a multi-sensory approach," in *Proc. 2000 IEEE Int. Conf. Robot. Autom.*, 2000, pp. 3687–3694.

[6] D. Lee, J. Kim, I. Kim, and M. Hahn, "Virtual assembly system for robot actor in performing art," *Int. J. Softw. Eng. Appl.*, vol. 8, pp. 339–350, Aug. 2014.

[7] A. E. Jimenez-Cano, J. Martin, G. Heredia, A. Ollero, and R. Cano, "Control of an aerial robot with multi-link arm for assembly tasks," in *Proc. 2013 IEEE Int. Conf. Robot. Autom.*, May 2013, pp. 4916–4921.

[8] J. W. Choi, T. H. Fang, W.-S. Yoo, and M. H. Lee, "Sensor data fusion using perception net for a precise assembly task," *IEEE Trans. Mechatronics*, vol. 8, no. 4, pp. 513–516, Dec. 2003.

[9] J. W. Choi, T. H. Fang, W.-S. Yoo, and M. H. Lee, "A model of shared grasp affordances from demonstration," in *Proc. IEEE-RAS Int. Conf. Humanoids Robots*, 2007, pp. 27–35.

[10] D. Silver, J. A. Bagnell, and A. Stentz, "Learning from demonstration for autonomous navigation in complex unstructured terrain," *Int. J. Robot. Res.*, vol. 29, no. 12, pp. 1565–1592, Jun. 2010.

[11] U. Nehmzow, O. Akanyeti, C. Weinrich, T. Kyriacou, and S. A. Billings, "Robot programming by demonstration through system identification," in *Proc. 2007 IEEE/RSJ Int. Conf. Intell. Robots Syst.*, 2007, pp. 801–806.

[12] J. Aleotti, S. Caselli, and M. Reggiani, "Toward programming of assembly tasks by demonstration in virtual environments," in *Proc. 2003 IEEE Int. Workshop Robot Human Interactive Commun.*, 2003, pp. 309–314.

[13] G. Smoljkic, G. Borghesan, D. Reynaerts, J. D. Schutter, J. V. Sloten, and E. V. Poorten, "Constraint-based interaction control of robots featuring large compliance and deformation," *IEEE Trans. Robot.*, vol. 31, no. 5, pp. 1252–1260, Oct. 2015.

[14] J. Takahashi, T. Fukukawa, and T. Fukuda, "Passive alignment principle for bobotic assembly between a ring and a shaft with extremely narrow clearance," *IEEE/ASME Trans. Mechatronics*, vol. 21, no. 1, pp. 196–204, Feb. 2016.

[15] C. C. Cheah, M. Hirano, S. Kawamura, and S. Arimoto, "Approximate Jacobian robot control with uncertain kinematics and dynamics," *IEEE Trans. Robot. Autom.*, vol. 19, no. 4, pp. 692–702, Aug. 2003.

[16] L. Cheng, Z. G. Hou, and M. Tan, "Adaptive neural network tracking control for manipulators with uncertain kinematics," *Dyn. Actuator Model*, vol. 45 pp. 2312–2318, 2009.

[17] M. R. Soltanpour, J. Khalilpour, and M. Soltani, "Robust nonlinear control of robot manipulation with uncertainties in kinematics, dynamics, and actuator models," *Int. J. Innov. Comput., Inf. Control*, vol. 8, pp. 5487–5498, 2012.

[18] H. Chen, C. Wang, X. J. Li, and D. Sun, "Transportation of multiple biological cells through saturation-controlled optical tweezers in crowded microenvironments," *IEEE/ASME Trans. Mechatronics*, vol. 21, no. 2, pp. 888–899, Apr. 2016.

[19] H. Chen and D. Sun, "Moving groups of microparticles into array with a robot-tweezers manipulation system," *IEEE Trans. Robot.*, vol. 28, no. 5, pp. 1069–1080, Oct. 2012.

[20] H. Qiao and S. K. Tso, "Three-step precise robotic peg-hole insertion operation with symmetric regular polyhedral objects," *Int. J. Prod. Res.*, vol. 37, pp. 3541–3563, 1999.

[21] H. Qiao, "Two-and three-dimensional part orientation by sensor-less grasping and pushing actions: Use of the concept of 'attractive region in environment'," *Int. J. Prod. Res.*, vol. 41, pp. 3159–3184, 2003.

[22] H. Qiao, M. Wang, J. H. Su, S. X. Jia, and R. Li, "The concept of 'attractive region in environment' and its application in high-precision tasks with low-precision systems," *IEEE/ASME Trans. Mechatronics*, vol. 20, no. 5, pp. 2311–2327, Oct. 2015.

[23] H. T. Cheng and H. P. Chen, "Online parameter optimization in robotic force controlled assembly processes," in *Proc. 2014 IEEE Int. Conf. Robot. Autom.*, 2014, pp. 3465–3470.

[24] B. L. Wu, D. K. Qu, and F. Xu, "Improving efficiency with orthogonal exploration for online robotic assembly parameter optimization," in *Proc. 2015 IEEE Int. Conf. Robot. Biomimetics*, 2015, pp. 958–963.

[25] H. P. Chen, B. B. Li, D. Gravel, G. Zhang, and B. Zhang, "Robot learning for complex manufacturing process," in *Proc. 2015 IEEE Int. Conf. Ind. Technol.*, 2015, pp. 3207–3211.

[26] M. L. Gredilla, J. Q. Candela, C. E. Rasmussen, and A. R. Vidal, "Sparse spectrum Gaussian process regression," *J. Mach. Learn. Res.*, vol. 11, pp. 1865–1881, Mar. 2010.
[27] J. Yuan, K. S. Wang, T. Yua, and M. L. Fang, "Reliable multi-objective optimization of high-speed WEDM process based on Gaussian process regression," *Int. J. Mach. Tools Manuf.*, vol. 48, pp. 47–60, Jan. 2008.
[28] D. N. Tuonga, M. Seegerb, and J. Petersc, "Model learning with local Gaussian process regression," *Adv. Robot.*, vol. 23, pp. 2015–2034, Apr. 2012.
[29] T. L. Zobrist, J. H. Burge, W. B. Davison, and H. M. Martin, "Measurements of large optical surfaces with a laser tracker," *Proc. SPIE*, vol. 7018, Jul. 2008, Art. no. 70183U.
[30] A. Nubiola and I. A. Bonev, "Absolute calibration of an ABB IRB 1600 robot using a laser tracker," *Robot. Comput.-Integ. Manuf.*, vol. 29, pp. 236–245, 2013.

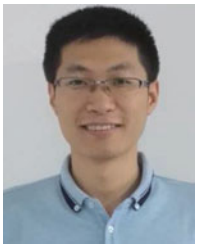

An Wan received the B.E. degree in mechanical engineering from Tsinghua University, Beijing, China, in 2011. He is currently working toward the Ph.D. degree in the Department of Mechanical Engineering, Tsinghua University.

His research interests include large-scale dimensional measurement and intelligent robotics.

Jing Xu (M'12) received the B.E. degree in mechanical engineering from the Harbin Institute of Technology, Harbin, China, in 2003, and the Ph.D. degree in mechanical engineering from Tsinghua University, Beijing, China, in 2008.

He was a Postdoctoral Researcher in the Department of Electrical and Computer Engineering, Michigan State University, East Lansing, MI, USA. He is currently an Associate Professor with the Department of Mechanical Engineering, Tsinghua University. His research interests include vision-guided manufacturing, image processing, and intelligent robotics.

Heping Chen (M'00–SM'05) received the B.S. degree in control system engineering from the Harbin Institute of Technology, Harbin, China, in 1989; the M.E. degree in electrical and electronic engineering from Nanyang Technological University, Singapore, in 1999; and the Ph.D. degree in electrical and computer engineering from Michigan State University, East Lansing, MI, USA, in 2003.

He was at Robotics and Automation Labs, ABB Corporate Research, ABB, Inc., Windsor, CT, USA, from 2005 to 2010. He is currently an Assistant Professor with the Ingram School of Engineering, Texas State University-San Marcos, San Marcos, TX, USA. His research interests include micro/nanomanufacturing, micro/nanorobotics, industrial automation, control system design, and implementation.

Song Zhang received the B.S. degree in mechanical engineering from the University of Science and Technology of China, Hefei, China, in 2000, and the M.S. and Ph.D. degrees in mechanical engineering from Stony Brook University, Stony Brook, NY, USA, in 2003 and 2005, respectively.

He is currently an Associate Professor in mechanical engineering with Purdue University, West Lafayette, IN, USA. His current research interests include developing superfast super-resolution 3-D imaging technologies and exploring their applications, 3-D machine/computer vision, biophotonic imaging, virtual reality, augment vision, human–computer interactions, forensic science, and biomedical engineering.

Ken Chen received the B.S. degree in mechanical engineering from Sichuan University, Chengdu, China, in 1982, and the M.S. and Ph.D. degrees in mechanical engineering from Zhejiang University, Hangzhou, China, in 1984 and 1987, respectively.

From 1991 to 1992, he was a Visiting Professor at the University of Illinois at Chicago, Chicago, IL, USA. From 1992 to 1995, he was a Postdoctoral Researcher at Purdue University, Indianapolis, IN, USA. He is currently a Professor with the Department of Mechanical Engineering, Tsinghua University, Beijing, China. His research interests include robotics and intelligent control, humanoid robots, microrobots and small robots, medical and space robots, manufacturing automation systems, and hydraulic servo systems.